Sociedade Brasileira de Automática (SBA)
XXV Congresso Brasileiro de Automática - CBA 2024, 15 a 18 de outubro de 2024

Static and Dynamic Aspects of the Power Interchange Between Areas

Fernanda Rippel Tonial * **Katia Campos de Almeida** **
Roberto de Souza Salgado ***

* *CPFL Energia, Campinas, SP, (e-mail: fer.tonial@hotmail.com).*
** *Depto. de Engenharia Elétrica e Eletrônica, Universidade Federal de Santa Catarina, (e-mail: katia.c.almeida@ufsc.br)*
*** *Depto. de Engenharia Elétrica e Eletrônica, Universidade Federal de Santa Catarina,(e-mail: roberto.salgado@ufsc.br)*

Abstract: Large power networks are generally divided in areas through which the power is transferred. Therefore, the determination of power flow solutions constrained by area interchange limits is important, since it allows to estimate the maximum amount of energy that can be interchanged under safe conditions. This work is focused on the study of the active power interchange in a multi-area electrical network, by adopting a procedure based on two steps:(i) the use of Optimal Power Flow (OPF) models to determine steady state power flow solutions taking into account the power interchange, and (ii) the assessment of these solutions from the point of view of Small Signal Stability. Numerical results obtained with a 68-bus power system illustrate the main features of the proposed approach.

Keywords: active power interchange, multi-area networks, optimal power flow, stability analysis, small disturbance

1. INTRODUCTION

Difficulties in transferring large blocks of power throughout the system arise as a consequence of, for example, unavailability of generation units, integration of intermittent energy sources, unforeseen contingencies or transmission limits in tie lines. These periods of power system stress could be alleviated through the integration of the electric grid, aimed at efficiently sharing power resources through the interconnections between well-defined areas (Department of Energy (2021)). The amount of power interchange must be compatible with operational security standards, which requires to identify the limits of the power supply considering both steady state and dynamic behaviour

The simplest methodologies to estimate the limits of power interchange are based on the conventional power flow solutions. Usually these procedures are time consuming due to the way of representing some operational conditions. Other approaches propose the inclusion of the interchange constraints into the power flow analytical formulation (Santos et al. (2004); Sotelo-Martinez and Fuerte-Esquivel (2017)), to calculate the loadability margin with simultaneous estimation of the maximum power transfer through the continuation power flow (Carhullanqui et al. (2015)). These models lack a well defined adjustment of the power system controls to cope with both the power transfer and the operational limits. Alternatively, the maximum power interchange can be estimated with the aid of OPF models, as proposed by Sant'Anna et al. (2009), which combine the flexibility to choose the index to be optimised and the possibility of including any steady state constraint in the analytical formulation, thus considerably improving the quality of the operational solutions.

An essential complement of the power interchange study is the analysis of the dynamic aspects of the steady state solutions. The transfer of large amounts of energy has considerable influence on the power system stability, specially the damping of electromechanical oscillations. Linearised models allow the study of steady-state solutions in the context of small signal stability (Dussaud (2015)). A recent paper (Yang et al. (2021)) proposes an optimisation model based on an equivalent two-machine system, which is solved by particle swarm optimisation, and uses Phasor Measurement Unity data to assess the inter-area transfer capability. When nonlinear models are required, the maximum power transfer can be calculated through electromechanical transient simulation (Sant'Anna et al. (2009)). Due to the repeated simulations required to determine the inter-area transfer limit, this type of procedure could be computationally burdensome and time consuming. Thus, Hou and Vittal (2013) propose the use of sensibility relationships related to the active power generation to estimate the limit of active power transfer under transient stability constrains.

This paper analyses static and dynamic aspects of power interchange between areas. For steady state analysis, the following Optimal Power Flow models are presented: (i) the maximisation of the active power net interchange without pre-specified change direction, (ii) maximization of active power interchange via parameterisation taking into account a pre-specified power change rate between the interconnections; (iii) the maximisation of the power

⋆ The authors are grateful to CNPq and CAPES for supporting this research.

demand with net interchange constraints, and; (iv) the minimisation of the squared deviation of the active power generation level with pre-specification of active power net interchange. The models take into account the power interchange between areas alternatively as a performance index or as an equality constraint. The solutions produced by the first two models can be considerably different, with distinct impacts on the dynamic of the network operation. The third model shows the interdependence between the pre-specified power interchange and the loadability level of the power system. The fourth formulation indicates the compromise between changes in active power generation and the active power interchange. These models are analytically represented by non-linear OPF problems, in which the loads are modelled as constant power and bus voltages are expressed in rectangular coordinates. These problems are solved through the Primal-Dual Interior Point method.

The complementary aspect of the proposed methodology is the assessment of the OPF results from the point of view of Small Signal Stability. This is accomplished with the aid of the academic version of the computational software PacDyn (CEPEL (2018)). Tests with an equivalent practical system indicate that the parameterised power interchange models produce steady state solutions with smaller impact in the power system dynamic stability, which can be attributed to the moderate changes in the power system variables resulting from the parameterisation scheme.

The remainder of this paper is organised as follows. The OPF models are described in Section 2. The basic theoretical concepts of Small Signal Stability used in this work are summarised in Section 3. Numerical results are analised in Section 4. Section 5 summarises the main conclusions of the approach.

2. OPTIMAL POWER FLOW WITH POWER INTERCHANGE

For the sake of simplicity, the power flow limits and the transformer taps are omitted in the following OPF formulations, though they have been considered in the computational implementation. The optimization variables are the real and imaginary components of bus voltages, $\mathbf{e}$ and $\mathbf{f}$, active and reactive power generation, $\mathbf{P}_g$ and $\mathbf{Q}_g$, and variable transformer tap settings Tonial (2021).

2.1 Maximisation of the power interchange with no pre-specified variation rate

In this case, the OPF problem is written:

$$\begin{aligned} \text{Maximise } & P_t(\mathbf{e},\mathbf{f}) = \sum_{(i,j)\in\Omega} P_{ij}(\mathbf{e},\mathbf{f}) \\ \text{subject to } & \mathbf{0} = \mathbf{P}_g - \mathbf{P}_d - \mathbf{P}(\mathbf{e},\mathbf{f}) \\ & \mathbf{0} = \mathbf{Q}_g - \mathbf{Q}_d - \mathbf{Q}(\mathbf{e},\mathbf{f}) \\ & \mathbf{P}_g^m \le \mathbf{P}_g \le \mathbf{P}_g^M \\ & \mathbf{Q}_g^m \le \mathbf{Q}_g \le \mathbf{Q}_g^M \\ & \mathbf{V}^m \le \mathbf{V}(\mathbf{e},\mathbf{f}) \le \mathbf{V}^M \end{aligned} \tag{1}$$

where $P_t(\mathbf{e},\mathbf{f})$ is the net active power flow, $P_{ij}(\mathbf{e},\mathbf{f})$ is the power flow from bus i to bus j, Ω is the set of active power flows to be maximized. The equality constraints are the power balance equations of each bus, $\mathbf{P}(\mathbf{e},\mathbf{f})$, $\mathbf{Q}(\mathbf{e},\mathbf{f})$ and $\mathbf{V}(\mathbf{e},\mathbf{f})$ are respectively the power injections and the bus voltage magnitudes expressed in terms of $\underline{\mathrm{e}}$ and $\mathbf{f}$. The superscripts m and M refer to the minimum and the maximum limits, respectively. Note that, whereas the active power flows to be maximised are pre-specified, the change direction of these power flows is undefined a priori.

2.2 Maximisation of the power interchange with pre-specified variation rates

In this case, the change rate of the power interchange is pre-specified with the aid of a parametrisation strategy. The power flow interchange between areas a and b is:

$$P_{t_{ab}} = P_{t_{ab}}^0 + \rho^2 \Delta P_{t_{ab}}, \tag{2}$$

where $P_{t_{ab}}^0$ is the power flow interchange of the base case, the scalar ρ is the active power flow interchange parameter, and $\Delta P_{t_{ab}}$ is the change rate of the power interchange.

The parameterised OPF problem is written:

$$\begin{aligned} \text{Maximise } & \rho \\ \text{subject to } & \mathbf{0} = \mathbf{P}_g - \mathbf{P}_d - \mathbf{P}(\mathbf{e},\mathbf{f}) \\ & \mathbf{0} = \mathbf{Q}_g - \mathbf{Q}_d - \mathbf{Q}(\mathbf{e},\mathbf{f}) \\ & \mathbf{0} = \mathbf{P}_{int}^0 + \rho^2 \boldsymbol{\Delta}\mathbf{P}_{int} - \mathbf{P}_{int}(\mathbf{e},\mathbf{f}) \\ & \mathbf{P}_g^m \le \mathbf{P}_g \le \mathbf{P}_g^M \\ & \mathbf{Q}_g^m \le \mathbf{Q}_g \le \mathbf{Q}_g^M \\ & \mathbf{V}^m \le \mathbf{V}(\mathbf{e},\mathbf{f}) \le \mathbf{V}^M. \end{aligned} \tag{3}$$

where $\mathbf{P}_{int}^0$ is the vector of the pre-selected area interchanges of the base case; $\boldsymbol{\Delta}\mathbf{P}_{int}$ is the vector of the change rates; and $\mathbf{P}_{int}(\mathbf{e},\mathbf{f})$ is the vector of the area interchanges. It must be pointed out that the pre-specification of each change rate of vector $\boldsymbol{\Delta}\mathbf{P}_{int}$ is essential to define both direction and magnitude of the power flow variation, since the factor ρ^2 ensures the direction defined by this change rate. The problems stated by Eqs. (1) and (3) produce similar solutions only if: 1) the set of transmission lines of the performance index of former is the same of the equality constraint of the latter, and 2) the power flow change rate $\boldsymbol{\Delta}\mathbf{P}_{int}$ is specified according to the solution of Eq. (1).

2.3 Maximisation of the power load with power interchange constraints

For this purpose, the power demand is parameterised by the loadability factor α, as in (Irisarri et al. (1997)):

$$\begin{aligned} \mathbf{P}_d &= \mathbf{P}_d^0 + \alpha \mathbf{r}_p \\ \mathbf{Q}_d &= \mathbf{Q}_d^0 + \alpha \mathbf{r}_q, \end{aligned} \tag{4}$$

where $\mathbf{P}_d^0$ and $\mathbf{Q}_d^0$ are respectively the vectors with the active and reactive power demand of the base case, and $\mathbf{r}_p$ and $\mathbf{r}_q$ are the corresponding load change rates.

The analytical model of the OPF problem is:

$$\begin{aligned} \text{Maximise } & \alpha \\ \text{subject to } & \mathbf{0} = \mathbf{P}_g - (\mathbf{P}_d^0 + \alpha^2 \mathbf{r}_p) - \mathbf{P}(\mathbf{e},\mathbf{f}) \\ & \mathbf{0} = \mathbf{Q}_g - (\mathbf{Q}_d^0 + \alpha^2 \mathbf{r}_q) - \mathbf{Q}(\mathbf{e},\mathbf{f}) \\ & \mathbf{P}_g^m \le \mathbf{P}_g(\mathbf{e},\mathbf{f}) \le \mathbf{P}_g^M \\ & \mathbf{Q}_g^m \le \mathbf{Q}_g(\mathbf{e},\mathbf{f}) \le \mathbf{Q}_g^M \\ & \mathbf{V}^m \le \mathbf{V}(\mathbf{e},\mathbf{f}) \le \mathbf{V}^M \\ & \mathbf{0} = \mathbf{P}_{int}^{prg} - \mathbf{P}_{int}(\mathbf{e},\mathbf{f}), \end{aligned} \tag{5}$$

where, $\mathbf{P}_{int}^{prg}$ is the vector whose components are the pre-specified active power interchange between areas, and $\mathbf{P}_{int}(\mathbf{e},\mathbf{f})$ has been previously defined. Note that, except for the inclusion of the power interchange constraints, this problem is similar to the traditional model of load maximisation under operational conditions presented in (Irisarri et al. (1997)). Therefore, it highlights the dependence between the loadability and the power interchange.

2.4 Minimisation of the squared deviation of the active power generation level with power interchange constraints

This model provides solutions reflecting the balance between the pre-programmed levels of both active power generation and interchange. It is expressed as:

$$\begin{aligned}\text{Minimise}\quad & \frac{1}{2}[\mathbf{P}_g-\mathbf{P}_g^{ref}]^t\mathbf{D}_\alpha[\mathbf{P}_g-\mathbf{P}_g^{ref}]\\ \text{subject to}\quad & \mathbf{0}=\mathbf{P}_g-\mathbf{P}_d-\mathbf{P}(\mathbf{e},\mathbf{f})\\ & \mathbf{0}=\mathbf{Q}_g-\mathbf{Q}_d-\mathbf{Q}(\mathbf{e},\mathbf{f})\\ & \mathbf{P}_g^m\le\mathbf{P}_g\le\mathbf{P}_g^M\\ & \mathbf{Q}_g^m\le\mathbf{Q}_g\le\mathbf{Q}_g^M\\ & \mathbf{V}^m\le\mathbf{V}(\mathbf{e},\mathbf{f})\le\mathbf{V}^M\\ & \mathbf{0}=\mathbf{P}_{int}^{prg}-\mathbf{P}_{int}(\mathbf{e},\mathbf{f}),\end{aligned} \tag{6}$$

where $\mathbf{P}_g^{ref}$ is a vector whose components are the reference active power generation level; the non-zeros of the diagonal matrix $\mathbf{D}_\alpha$ are the weighting factors attributed to the active power deviation; $\mathbf{P}_{int}^{prg}$ is the vector of the pre-programmed active power interchanges, and $\mathbf{P}_{int}(\mathbf{e},\mathbf{f})$ has been previously defined.

3. SMALL SIGNAL STABILITY

An electrical power system can be analytically described by a set of differential algebraic equations (Kundur (1994)), expressed in compact form as:

$$\begin{aligned}\dot{\mathbf{x}} &=\mathbf{f}(\mathbf{x},\mathbf{z},\mathbf{u})\\ \mathbf{0} &=\mathbf{g}(\mathbf{x},\mathbf{z},\mathbf{u})\\ \mathbf{y} &=\mathbf{h}(\mathbf{x},\mathbf{z},\mathbf{u}),\end{aligned} \tag{7}$$

where $\mathbf{x}$ is the vector of the state variables, which are associated with the electrical and primary machines and respective controls; $\mathbf{z}$ and $\mathbf{u}$ are the vectors of the algebraic and the controllable variables, respectively, of the differential equations; $\mathbf{y}$ is the vector of the algebraic variables expressed in terms of the state and input variables, such as power flows in the transmission system, rotor speed of the synchronous generators etc.

The linearisation of Eq. (7) yields:

$$\begin{aligned}\dot{\mathbf{\Delta x}} &=\mathbf{A\Delta x}+\mathbf{B\Delta u}\\ \mathbf{\Delta y} &=\mathbf{C\Delta x}+\mathbf{D\Delta u},\end{aligned} \tag{8}$$

where $\mathbf{A}$, $\mathbf{B}$, $\mathbf{C}$ and $\mathbf{D}$ are matrices representing the first derivatives of Eqs. (7) with respect to the state, controllable and algebraic variables.

The modal analysis of the power system is based on the eigenvalues of the matrix $\mathbf{A}$, which can be real or complex numbers. The positive real numbers indicate the *monotonic instability* (Domingues (2005)), in which the absence of synchronising torque results in a continuous rotor angle increase. The complex eigenvalues are conjugate pairs corresponding to an oscillatory mode, with the positive real components pointing out the *oscillatory instability* (Domingues (2005)). In this case, the absence of damping torque results in oscillations with a steady and increasing amplitude (Kundur (1994)). The frequency of the electromechanical oscillations is in the range 0,1 to 2,0 Hz. These oscillations can be a *local mode* or an *inter-area mode* (Dussaud (2015)). The frequency of the latter is in the range between 0,1 and 0,7 Hz, while the oscillations of a local mode are in the frequency range of 0,7 to 2,0 Hz.

A pair of eigenvectors, denoted ϕ_i (*right*) and φ_i (*left*), is associated with each eigenvalue λ_i. They provide information about the possible reasons for weakly damped or unstable modes. For this purpose, the so-called *participation factors*, which indicate the sensitivity of the oscillation modes with respect to the state variables, are used. The participation factor corresponding to the n-th state variable in the critical mode i is expressed as the product (element-wise) of the eigenvectors associated with λ_i. Besides, the analysis of the right eigenvectors provides information about the behaviour of the state variables with respect to the excitation of a mode. This information is based on the so-called *mode shapes*, which is a diagram indicating the amplitude and the phase of the element ϕ_{n_i} of the right eigenvector matrix, corresponding to a mode i. The magnitude of ϕ_{n_i} reveals the degree of activity of each state variable in the i-th mode, whereas its angle provides the phase of each state variable with respect to the i-th mode.

4. NUMERICAL SIMULATION RESULTS

In order to assess the proposed methodology, the OPF formulations described in the previous sections have been computationally implemented in Matlab. In the first step of the proposed procedure, the OPF models provide solutions that optimise the power transfer between pre-specified areas while respecting physical/operational limits. In the subsequent step, these solutions are analysed with the aid of the computational software PacDyn (CEPEL (2018)), in order to verify their stability condition. The analysis of the dynamic aspects of the steady state solutions is based on the main eigenvalues; that is, those which correspond to inter-area oscillation modes and all critical or unstable eigenvalues. With the aim of checking if they actually indicate the inter-area oscillations, the corresponding mode shapes are analysed.

The single-line diagram of the test system used in the simulations is presented in Figure 1. This network represents the interconnection between the equivalent electrical power system of New England (USA), referred to as area 2, and the electrical network of New York (USA), referred to as area 1. The power import from each of the three other neighbouring areas are modelled as equivalent generator (G14, G15 and G16), corresponding to areas 3, 4 and 5, respectively. The system data can be found in (Ramos et al. (2014)) and (Singh and Pal (2013)). Regarding the dynamic data, all the generators were represented by model 5 of the synchronous machine (Kundur (1994)). According to (Ramos et al. (2014)) and (Singh and Pal (2013)), generators from 1 to 12 have Power System Stabilizers (PSS). Besides, the bus 16, which represents the angular reference, was modelled as an infinite bus.

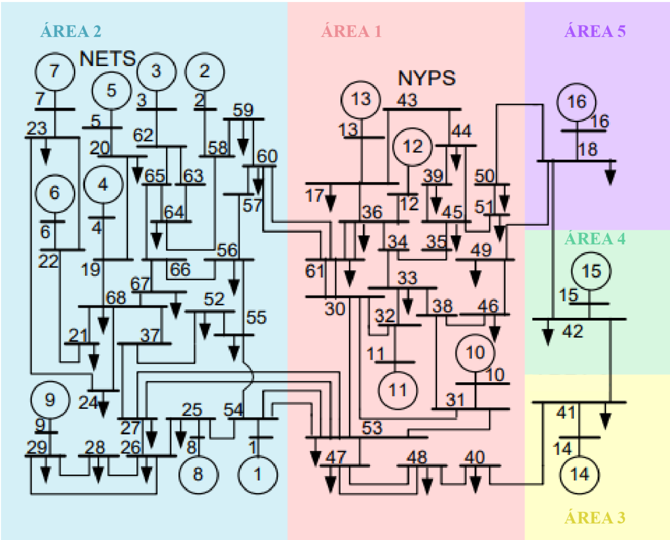

Fig. 1. New England/New York 68 bus network

The base case steady state solution was obtained through an OPF program that minimises the squared deviation from a pre-specified voltage magnitude level (Tonial (2021)). In the following, this case is denoted Case 0. This solution is basically the same solution presented in (Singh and Pal (2013)). The results provided by PacDyn concerning the small signal stability indicate a stable operation condition.

4.1 Minimisation of the net interchange of area 1

The OPF formulations (1) and (3) were used to increase the power import from area 1. The numerical results are summarised in tables 1 and 2. In the first table, columns 3, 4 and 5 indicate the active power flow in the interconnections for the base case (superscript(0)) and OPF formulations of Eqs. (1) and (3), with superscripts (1) and (3), respectively. The analysis of area 1 interconnections reveals that the formulation (1) provides greater values of active power imports. The smaller values corresponding to formulation (3) can be attributed to the use of the parameterisation scheme, which imposes the same change rate to the power flow in interconnections 2-1, 3-1 and 5-1; that is, an increase of 100,4% in the base case values.

Table 1. Minimisation of the net interchange of area 1 - Active power interchange

From (Area)	To (Area)	$P_{int}^{(0)}$ (MW)	$P_{int}^{(1)}$ (MW)	$P_{int}^{(3)}$ (MW)
1	2	-701,78	-2956,43	-1396,76
1	3	-473,62	-27,92	-911,02
1	5	-1038,05	-2252,60	-2056,06
4	3	-293,38	1069,41	-367,38
5	4	-142,55	948,96	-699,85

The active power generation and the active power net interchange of each area are presented in Table 2. In both cases, there is a reduction in the active power generation of area 1 (columns 4 and 6), in order to enable the increase of the active power import (columns 5 and 7).

Table 2. Minimisation of the net interchange of area 1 - Generation and net interchange

Area	$P_g^{(0)}$ (MW)	$\sum P_{int}^{(0)}$ (MW)	$P_g^{(1)}$ (MW)	$\sum P_{int}^{(1)}$ (MW)	$P_g^{(3)}$ (MW)	$\sum P_{int}^{(3)}$ (MW)
1	6441,00	-2213,45	3502,14	-5236,95	4314,04	-4363,84
2	5182,00	709,66	7733,83	3116,07	5900,68	1422,19
3	1785,00	785,00	0,01	1097,52	2350,15	610,71
4	1000,00	154,39	1302,84	-79,04	1500,00	-327,80
5	3377,50	907,50	5745,36	3274,83	3874,48	1404,49

Concerning the stability analysis, the eigenvalues corresponding to the solutions of problems (1) and (3) are presented in Table 3. It can be inferred that the solu-

Table 3. Minimisation of the net interchange of area 1 - Stability analysis

Without pre-specified change direction (1)			
Eigenvalue	f (Hz)	F_a (%)	F_p
-0,1369±j4,7975	0,7635	2,8518	WW BUS-15
0,08362±j2,5519	**0,4061**	**-3,2750**	**WW BUS-14**
0,1797±j3,1818	**0,5064**	**-5,6380**	**DELT BUS-13**
With pre-specified change direction (3)			
Eigenvalue	f (Hz)	F_a (%)	F_p
-0,3143±j3,7789	**0,6014**	**8,2886**	**WW BUS-13**
-0,07159±j2,0746	**0,3302**	**3,4488**	**WW BUS-14**
-0,1452±j5,0836	0,8091	2,8547	WW BUS-15

tion based on Eq. (1) represents an unstable operational condition. There are two eigenvalues with positive real part and negative damping factor (0,08362±j2,5519 and 0,1797±j3,1818), the smallest damping factor of which corresponding to an inter-area mode. These complex eigenvalues with positive real components correspond to oscillations with growing amplitudes, indicating a case of oscillatory instability. The variables with greater impact on these oscillations are the rotor speed of bus 14 (WW) and the rotor angle from bus 13 (DELT). The solution to the OPF model (3), although stable, is associated with two critical eigenvalues and damping factors under 5% (-0,07159±j2,0746 and -0,1452±j5,0836). Their corresponding participation factors indicate the rotor speed of buses 14 and 15 as the variables with greatest influence in the poorly damped oscillations. In this case, the eigenvalue with smallest damping factor has frequency greater than 0,7 Hz, although the analysis of its mode shapes reveals that it actually points out to another inter-area mode, as shown in Figure 2.

4.2 Maximisation of the net interchange of area 1

In this case, the maximum active power export from area 1 is sought. Thus, the solutions presented in tables 4 and 5 are also based on the formulations (1) and (3). Table 4 shows the active power interchanges. There are considerable differences between the results with respect of the direction of the power flow in the interconnections. In case of formulation (3), the change direction was defined by

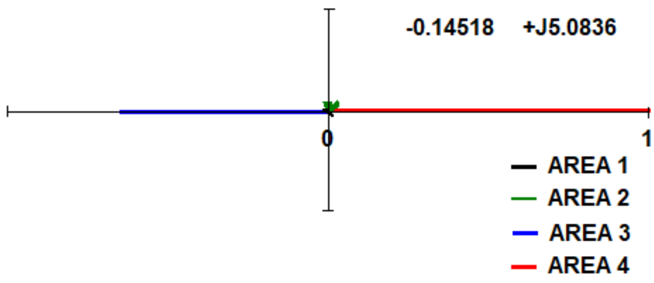

Fig. 2. Minimisation of the net interchange of area 1 - Mode Shapes

looking forward to increasing the active power flow leaving area 1.

Table 4. Maximisation of the net interchange of area 1 - Active power interchange

From (Area)	To (Area)	$P_{int}^{(0)}$ (MW)	$P_{int}^{(1)}$ (MW)	$P_{int}^{(3)}$ (MW)
1	2	-701,78	1827,41	314,92
1	3	-473,62	-813,08	212,54
1	5	-1038,05	-7,09	465,83
3	4	-293,38	812,71	101,45
4	5	-142,55	1132,45	-96,23

In the first row of Table 5, columns 5 and 7 indicate similar total net interchanges from area 1 (1007,25 MW and 993,29 MW), although there are considerable differences of active power generation of each area connected to area 1 (columns 4 and 6).

Table 5. Maximisation of the net interchange of area 1 - Generation and net interchange

Area	$P_g^{(0)}$ (MW)	$\sum P_{int}^{(0)}$ (MW)	$P_g^{(1)}$ (MW)	$\sum P_{int}^{(1)}$ (MW)	$P_g^{(3)}$ (MW)	$\sum P_{int}^{(3)}$ (MW)
1	6441,00	-2213,45	9661,50	1007,25	9661,50	993,29
2	5182,00	709,66	2692,13	-1773,17	4146,80	-309,38
3	1785,00	785,00	2677,50	1677,50	890,90	-108,75
4	1000,00	154,39	1500,00	350,00	953,34	-197,34
5	3377,50	907,50	1409,89	-1060,27	2104,56	-365,10

The results of the assessment of the dynamic aspects of these OPF solutions are presented in Table 6. In the upper part of this table, it is noticed that the solution based on Eq. (1) leads to an unstable condition, with a real positive eigenvalue (0,01961). Its participation factor indicates the quadrature axis transient internal voltage of bus 14 as the variable with greater influence in the oscillations. The additional critical eigenvalue (-0,1312±j4,2663) indicates that this instability corresponds to an inter-area mode. The lower part of Table 6 indicates that the solution based on Eq. (3) is stable. However, there are two critical eigenvalues (-0,1634±j5,2661 and -0,00708±j2,7191), the latter with considerably low damping (0,2605%). This can be seen a critical solution, where the system would spend a reasonable time to reach the steady state after a disturbance. Furthermore, in case of eventual uncertainties in the model, this condition could even be seen as unstable.

Table 6. Maximisation of area 1 net interchange - Stability analysis

Eigenvalue	f (Hz)	F_a (%)	Fp
Without pre-specified change direction (1)			
-0,1312±j4,2663	**0,6790**	**3,0747**	**DELT BUS-15**
0,01961	0	-100,00	EQ' BUS-14
With pre-specified change direction (3)			
-1,1408±j3,6462	**0,5803**	**29,861**	**WW BUS-13**
-0,1634±j5,2661	0,8381	3,1008	DELT BUS-15
-0,00708±j2,7191	**0,4328**	**0,2605**	**DELT BUS-14**

Figure 3 presents the mode shapes of the critical eigenvalues from the lower part of Table 6. At the top of this figure, which corresponds to the eigenvalue -0,00708±j2,7191, it is possible to identify the oscillations between two groups of generators, confirming the assumption that it corresponds to an inter-area mode. In the central and lower parts of the figure, which corresponds to the eigenvalue -0,1634±j5,2661, it is possible to see the oscillation of generator 15 against generator 14, also indicating the existence of inter-area oscillations.

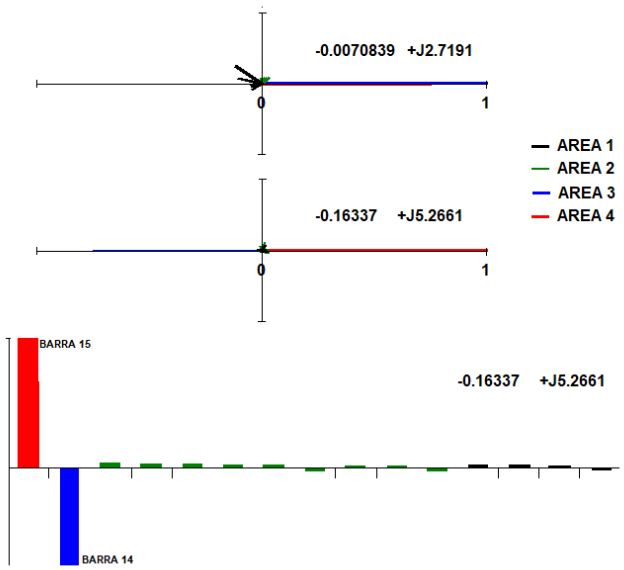

Fig. 3. Maximization of area 1 net interchange - Mode Shapes

In addition, the positive real eigenvalue indicates the monotonic instability, characterised by the continuous increasing of rotor angle (Domingues (2005)). Figure 4 illustrates the two cases of instability, presented in these last subsections. The upper part of this figure is the case of minimisation of the net interchange of area 1 without pre-specified change direction. It presents the variation of the active power generation after a small disturbance. The oscillations with increasing amplitudes confirm the case of oscillatory instability. The lower part of this figure refers to the maximisation of the net interchange of area 1 without

ISSN: 2525-8311

DOI: 10.20906/CBA2024/4325

pre-specified change direction. It shows the behaviour of the rotor angle after a small disturbance in the system. The exponential shape of these curves reveals their monotonic instability characteristic.

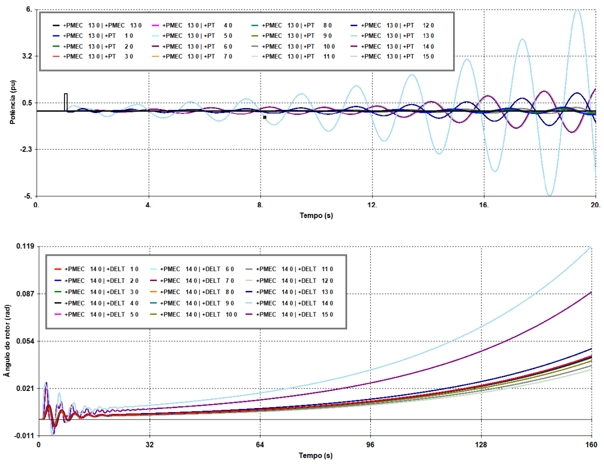

Fig. 4. Graphics - Unstable cases

4.3 Maximisation of the power demand of area 1

In this study, the maximum power demand of area 1 was determined under the following two conditions: 1) without taking into account active power interchange constraints; and 2) supposing the active power interchange of interconnections 1-2, 1-3 and 1-5 fixed at their base case values. The results obtained in these cases are based on the OPF model stated by Eq. (5) and referred to in this subsection as *unconstrained case* and *constrained case*, respectively. These solutions, which are denoted by the superscripts (5.1) and (5.2), respectively, are summarised in Tables 7 and 8. The former presents the power interchange for all interconnections in the base case (denoted (0), as previously) and in the last two cases mentioned.

Table 7. Maximisation of the power demand of area 1 - Active power interchange

From (Area)	To (Area)	$P_{int}^{(0)}$ (MW)	$P_{int}^{(5.1)}$ (MW)	$P_{int}^{(5.2)}$ (MW)
1	2	-701,78	-3034,81	-701,78
1	3	-473,62	-882,65	-473,62
1	5	-1038,05	-2702,76	-1038,05
3	4	296,94	183,86	414,21
4	5	143,38	146,81	101,85

Table 8 shows that the solution to (5.1) yields an increase of 84,4% in the loadability of area 1, which requires a corresponding increase in the net interchange of area 1 from -2214,08 MW (base case) to -6620,22 MW. On the other hand, the inclusion of interchange constraints (solution (5.2)), restrains the loadability increase to 36,9%, which is completely supplied by the internal generation of area 1, since the power interchange in unchanged with respect to the base case values.

Table 8. Maximisation of the power demand of area 1 - Generation and load

Area	$P_g^{(0)}$	$P_g^{(5.1)}$	$P_g^{(5.2)}$	$P_d^{(0)}$	$P_d^{(5.1)}$	$P_d^{(5.2)}$
1	6441,00	9661,15	9661,28	8574,93	15812,01	11738,64
2	5182,00	7771,85	5179,14	4425,80	4425,80	4425,80
3	1785,00	2129,40	1899,93	1000,00	1000,00	1000,00
4	1000,00	1114,80	844,39	1150,00	1150,00	1150,00
5	3377,50	5131,09	3418,14	2470,00	2470,00	2470,00
Total	17785,50	27609,8	2472,58	7213,72	17620,73	27258,43

The results of the stability analysis of these solutions are summarised in Table 9. In the unconstrained case, there is a complex eigenvalue (0,1298±j4,1146) related to an oscillatory instability, indicating the rotor speed of bus 13 as the main responsible for this unstable characteristic. There are other two critical eigenvalues. The first corresponds to a local mode (-0,1632±j4,9533) and the second is related to an inter-area mode (-0,06874±j2,1576). The constrained OPF solution is stable, with a critical eigenvalue (-0,1699±j4,9789). In this case, the less damped eigenvalue corresponds to a local mode, while the other eigenvalues correspond to inter-area oscillations.

Table 9. Maximisation of the power demand of area 1 - Stability analysis

Unconstrained case (5.1) (			
Eigenvalue	f (Hz)	F_a (%)	F_p
-0,1632±j4,9533	0,7883	3,2923	WW BUS-15
-0,06874±j2,1576	**0,3434**	**3,1844**	**WW BUS-14**
0,1298±j4,1146	**0,6549**	**-3,1527**	**WW BUS-13**
Constrained case (5.2)			
Eigenvalue	f (Hz)	F_a (%)	F_p
-0,5135±j4,0306	**0,6415**	**12,637**	**WW BUS-13**
-0,1424±j2,5898	**0,4122**	**5,4892**	**WW BUS-14**
-0,1699±j4,9789	0,7924	3,4107	WW BUS-15

4.4 Minimum deviation OPF solutions

To conclude this stability study, the OPF solutions based on formulation (6) were analysed. In this case, the target is to find the minimum adjustment in the active power generation in order to satisfy the simultaneous variations in both power load and power interchange of area 1. For this purpose, the results presented in tables 1 and 4 (minimisation and maximisation with pre-specified variation direction) were adopted as references to pre-specify the variations.

In the first case, net interchange of area 1 was modified from -2213.45 MW (base case, 3rd column of Table 1) to 272,20 MW (a variation of 123%). Simultaneously, the power demand of area 1 (8574.93 MW in the base case) was increased in 8,58%, to 9310,66 MW. In the second case, interchanges 1-2 and 1-3 were maintained in their minimum values (5th column of Table 1), while interchange 1-5 was increased in 57,7% of its base case value (3rd column of Table 1). Simultaneously, the load of area 1 was increased in 40%, to 12004,90 MW. The resulting net interchange was -3992,81 MW.

Table 10 summarizes the results corresponding to both conditions. Columns 2 and 3, 4 and 5, 6 and 7 show respectively the active power generation, the interchange and the demand, as well as their corresponding variations with respect to the base case.

Table 10. Minimization of the squared deviation of the active power generation level - Summary of the two solutions

Area 1	P_g	ΔP_g	P_{int}	ΔP_{int}	P_d	ΔP_d
Solution 1	9643,35	3202,35	272,20	2485,65	9310,66	735,73
Solution 2	8252,33	1811,33	-3992,81	-1779,36	12004,90	3429,97

The stability analysis of these solutions is presented in Table 11. It is shown that the solution 1 is stable whilst the solution 2 is monotonically unstable, with real positive eigenvalue 0,02388. Figure 5 confirms this instability case, presenting the variation of the rotor angle after a small disturbance. In this case, the quadrature axis transient internal voltage of bus 14 is the variable with greatest influence in the unstable oscillations. Further studies beyond the scope of this paper would be necessary to verify aspects of this solution eventually related to voltage instability.

Table 11. Minimization of the squared deviation of the active power generation level - Stability analysis

Solution 1			
Eigenvalue	f (Hz)	F_a (%)	F_p
-0,9696±j3,7572	**0,5980**	**24,987**	**WW BUS-13**
-0,1099±j2,4889	**0,3961**	**4,4105**	**DELT BUS-14**
-0,1418±j4,3291	0,6890	3,2747	WW BUS-15
Solution 2			
Eigenvalue	f (Hz)	F_a (%)	F_p
-0,2093±j4,1662	**0,6631**	**5,0183**	**DELT BUS-13**
-0,1440±j4,4219	0,7038	3,2538	WW BUS-15
0,02388	0	-100,00	EQ' BUS-14

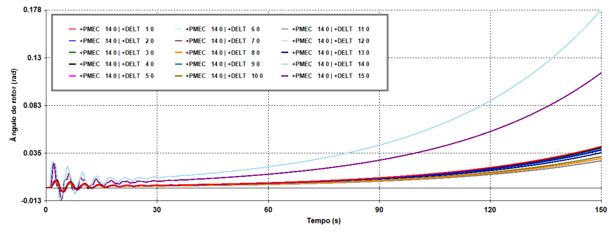

Fig. 5. Minimization of the squared deviation of the active power generation level - Unstable case

5. CONCLUSION

The methodology proposed in this paper analyses both static and dynamic aspects of solutions obtained via different OPF models. It points out several important differences between these operating conditions, which could be essential to establish the power system controls. The OPF models provide distinct solutions for the problem of controlling power interchange between areas, which have different behaviour from the point of view of small signal stability. The numerical simulation with an equivalent real network indicate that the parameterised models produce solutions with a smaller impact on the dynamic aspects of the power system operation, from the point of view of small disturbances. This could be attributed to the moderate changes resulting from the parameterisation. Future work points to the inclusion of stability indexes in the OPF models.

REFERENCES

Carhullanqui, H.A., Neto, A.B., and Alves, D.A. (2015). Continuation power flow considering area net interchange constraint. *International Journal of Electric Power and Energy Systems*, 70, 118–126.

CEPEL (2018). *User's Manual.* Centro de Pesquisas de Energia Elétrica.

Department of Energy (2021). *Uniting the U.S. Power System.* Spring 2021 RD Newsletter. URL `https://www.energy.gov/eere/wind/articles/uniting-us-power-system`.

Domingues, A.F. (2005). *Um modelo de espaço de estados com representação de segunda ordem para análise das oscilações de modo interárea em sistemas de energia Elétrica.* Ph.D. thesis, Universidade Estadual de Campinas, Campinas, SP.

Dussaud, F. (2015). *An application of modal analysis in electrical power systems to study inter-area oscillations.* Master's thesis, KTH Royal Institute of Science and Technology, School of Electrical Engineering, Stockholm, Sweden.

Hou, G. and Vittal, V. (2013). Determination of transient stability constrained interface real power flow limit using trajectory sensitivity approach. *IEEE Transactions on Power Systems*, 28(3), 2156–2163. doi:10.1109/TPWRS.2012.2222942.

Irisarri, G.D., Wang, X., Tong, J., and Mokhtari, S. (1997). Maximum loadability of power systems using non linear interior point method. *IEEE Transactions on Power Systems*, 12(1), 162–172.

Kundur, P. (1994). *Power System Stability and Control.* McGraw-Hill, Inc.

Ramos, R.A., Kuiava, R., Fernandes, T.C.C., Pataca, L.C., and Mansour, M.R. (2014). *IEEE PES Task Force on Benchmark Systems for Stability Controls.*

Sant'Anna, E.G.S., Souza, A.C.Z., Takahata, A.Y., Schilling, M.T., and Filho J. A., P. (2009). Cálculo de limites de intercâmbio em sistemas de grande porte através de ferramentas de otimização. In *XI Symposium of specialists in electric operational and expansion planning.*, 1–6.

Santos, M.J., Pereira, J.L.R., Passos Filho, J.A., Oliveira, E.J., and Silva Jr., I.C. (2004). A new approach for area interchange control modelling. *IEEE Transactions on Power Systems*, 19(3), 1271–1276.

Singh, A.K. and Pal, B.C. (2013). *IEEE PES Task Force on Benchmark Systems for Stability Controls.*

Sotelo-Martinez, J.A. and Fuerte-Esquivel, C.R. (2017). A new practical area interchange control model for power flow studies. *IEEE Transactions on Power Systems*, 32(3), 162–172.

Tonial, F.R. (2021). *Aspectos Estáticos e Dinâmicos das Soluções do FPO com Inclusão de Restrições de Intercâmbio de Potência.* Master's thesis, Universidade Federal de Santa Catarina.

Yang, D.Y., Wang, L., Cai, G., Chen, Z., Ma, J., Wang, B., and Sun, Z. (2021). Synchronized ambient output-only based online inter-area transfer capability assessment considering small signal stability. *IEEE Transactions on Power Systems*, 36(1), 261–270. doi:10.1109/TPWRS.2020.3004838.